Improved observer dependent perception of weak edges when scanning an image in real time indicated by introducing 1/f noise into the primary visual cortex V1. Theory and experimental support

E. Thornton-Benko[1], H. T. Nguyen[2], W. T. Hung[3] and B. S. Thornton[4]

[1]*Royal Prince Alfred Hospital, Camperdown, Sydney, Australia*
[2]*Key Centre for Health Technologies, University of Technology, Sydney, Australia*
[3]*Breast Screen, New South Wales, Australia*
[4]*School of Physics University of Sydney, Australia and Department of Mathematics, University of Technology Sydney, Sydney, Australia*

Abstract

We present results of a new process for generating $1/f$ type noise sequences and introducing the noise in the primary visual cortex which then enables improved perception of weak edges when an observer is scanning a complex image in real time to detect detail such as in mammogram reading sessions. It can be explained by an adaptation of information theory for functional rather than previous task-based methods for formulating processes for edge formation in early vision. This is enabled from a two "species" classification of the interaction of opposing on-centre and off-centre neuron processes. We show that non-stationary stochastic resonances predicted by theory can occur with $1/f$ noise in the primary visual cortex V1 and suggest that signalling exchanges between V1 and the lateral geniculate nucleus (LGN) of the thalamus can initiate neural activity for saccadic action (and observer attention) for weak edge perception. Improvements predicted by our theory were shown from 600 observations by two groups of observers of limited experience and an experienced radiologist for reference (but not for diagnosis). They scanned and rated the definition of microcalcification in clusters separately rated by the experienced radiologist. The results and supporting theory showed dependence on the observer's attention and orderly scanning. Using a compact simplified equipment configuration the methodology has important clinical applications for conjunction searches of features and for detection of objects in poor light conditions for vehicles.

Key words edge detection, $1/f$ noise, Lotka-Volterra equations, information theory, stochastic resonances

Introduction

There is a need in many disciplines to improve observer perception of weak edges when scanning images for detail. This is the case, for example, in mammography when scanning sequences of screened breast images in real-time conditions for suspect signs of early breast cancer. Training needs for such applications prompted the work in the present report for a method to improve edge detection of weakly defined shapes and edges having variations in optical density. In our context the term "weak edge" relates to a low value of the spatial gradient at what, to the observer, appears to be a low contrast boundary of an object in a breast mammogram image. Regular grid image patterns were initially considered but were not realistic for the practical medical situations of interest. Microcalcification deposits often occurring as clusters in mammograms are sometimes easy to notice but it is the foregoing parameters and spatial distribution (including any outlying deposits or embedded in areas of dense parenchymal tissues) which are important. The aim was to improve edge responses in an observer's vision system when scanning such images in real time conditions. We used basic characteristic examples from a hospital data base which we had previously quantified to establish a reference base by a fractal method which includes the size, shape, density and distribution. The values were compared with ratings by an experienced radiologist and found to be consistent for the range 1 to 5

Corresponding author: Elysia Thornton-Benko Royal Prince Alfred Hospital, Camperdown, Sydney, Australia
Email: fthornton@ozemail.com.au, Tel: +61 2 9879 4126

for edge quality definition based on the foregoing properties. The expert requirement of difficult diagnostic interpretation methods in our other projects[1] was not involved in those particular experiments.

Stochastic resonance (SR) from random Gaussian noise has been shown to occur in the cortex for improved observer recognition of intensity change in a harmonically varying patch of illumination of progressively declining intensity produced on an observer's computer screen[2]. The periodic small patch of declining illumination was added to that of only one eye, shielded from the other, and the two eye inputs were combined at V1. However, although that experiment indicated that SR was acting in the cortex, the neurology for observer perception of individual edges in an image is quite different. This will be seen in this present paper from a "two species" based Lotka-Volterra formulation of on-centre and off-centre neuron group interactions for edge response.

We show that functional information processes for edge formation by on-centre excitatory and off-centre inhibitory neurons in the primary vision pathway when treated in terms of "two species" yields Lotka Volterra (LV) type equations for the excitatory and inhibitory ganglion responses from which an edge response is produced for approximately equal values at particular threshold levels of intensity. We show that the LV type of differential equations also apply for the introductions at V1. We introduce $1/f$ noise to interact at V1 with each of the two neuron species because it has previously been shown[3] that $1/f$ type noise is required for stochastic resonances to occur from the interaction of the variables in LV differential equations. Signalling information exchanges between V1 and the lateral geniculate nucleus (LGN) can relay the responses at V1 to the cortical front eye field (FEF) via the thalamus[4] and produce saccadic action for an observer attention when scanning an image as indicated from our experiments.

$1/f$ noise, is a frequency deformation with power spectrum correlations of a white noise spectrum. The power spectrum decay is $1/f^{\alpha}$ with $0<\alpha<2$. It has the surprising ability to produce resonances of subthreshold signals in nonlinear processes. Wide ranging examples occur in nature, biological and other applications including those of cellular membrane potentials[5] heart beats[6] and brain electromagnetics[7]. The origins of $1/f$ fluctuations in nature are not fully known. We generated $1/f$ for our observer experiments using the system shown in Fig 1 (described in detail in a subsequent Section) which utilises polarised random white noise segments and selective polaroid filters for the correlated spectral responses of the retinal rods and cones of each eye to provide power spectrum correlations of the white noise spectrum.

Although individual neurons are noisy this does not affect normal everyday vision. Neural encoding at the group population level of two species when correlated activity is considered and where spiking of neighbouring neurons is taken into account has recently been shown[8] to be less noisy than would be expected from the variability of

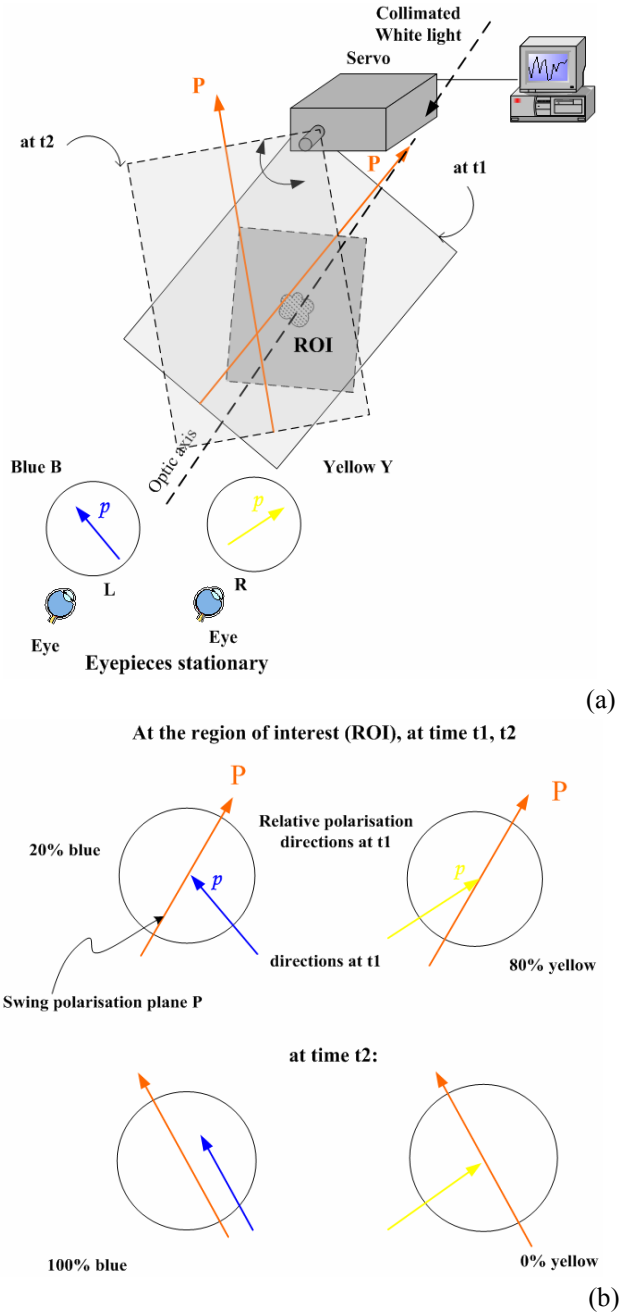

Figure 1. *(a) $1/f$ noise generation principle for dynamic optical/neurological retinal system uses a computer driven swinging polaroid in small random time steps of white noise over the variable swing time t of the order $0.1s$. The steps across optic axis provides independent random inputs to the orthogonally polaroid eyepiece filters. Both have 3 different maxima and minima of differing levels (analogous to resonant circuits) in the blue (left eye) and yellow (right eye) spectral regions. Retinal input via the correlated spectral absorption spectra of rods and cone receptors provides the correlated $1/f^2$ (approx) power spectra required for $1/f$ noise in yellow $650nm$ to blue $400nm$ region. Retinal illumination approx $30cd\,m^{-2}$. (b) Relative polaroid axes and colour mix from dynamic polaroid P at t_1 and t_2 with respect to fixed axes of left and right eye polaroids and filters.*

individual neurons. Also 20% additional information is extracted from the visual scene than by assuming independence and 40% more information is preserved than optimal linear coding.

The paper is presented as follows:

We begin with the basic theory which provides the background leading to the experiments including a brief outline of the early vision system involved in edge formation where we use the "two species" functional approach for the role of the neurological on-centre and off-centre opposing signals. This then allows formulation in terms of the well known Lotka-Volterra differential equations as detailed in later sections with Figs 3 and 4. We then describe the reference set of images and selection of observers. We then describe the laboratory generation of $1/f$ noise for testing the hypothesis of improved weak edges by introducing $1/f$ noise into the observer's vision system. The observer tests used two sets of observers of the reference set of images which had ratings (1 – 5) for perception of detail done by an experienced radiologist. Results of the observer tests are then presented. Supporting theory for the modelling expands on the basic theory given previously and provides the key features related to observer results. An orbital representation of non- stationary and improved on-centre and off-centre responses and its relevance to observer's scanning performance is then demonstrated graphically in 3D. Discussion and Conclusions include practical aspects for observers in edge recognition in clinical applications and further developments.

Theoretical background

The primary visual pathway begins at the retina and involves the lateral geniculate nucleus

(LGN) and the visual cortex V1. A greatly simplified illustration of the visual pathways is shown in Fig 2. The LGN is a small but very important part $(\approx 1.5$ million cells) of the thalamus in the pathway for each eye. Retinal ganglions receive spatial information in the form of excitatory ("light") and inhibitory ("dark") signals to form an edge and transmit this information via action potential spike pulses to the separate layers of the LGN. Each LGN relays signals to the visual cortex V1 but it also is involved with extensive signals back-projected from the cortex and associated neurological processes, not all of which are known in their exact functions.

The formation of a perceived edge in the vision system results from the interaction in the primary visual cortex V1 of the excitatory and inhibitory signals from the repetitive action of the potential discharges (spikes) initiated respectively from the local on-centre (excitatory) and off-centre (inhibitory) receptive fields of retinal ganglions. As a result the image of the edge at V1 is formed. Such a "two species" competitive process can be represented by the Lotka-Volterra type of differential equations (de's) which arose initially for coexisting predators and prey interactions. A good exposition of the topic is given by

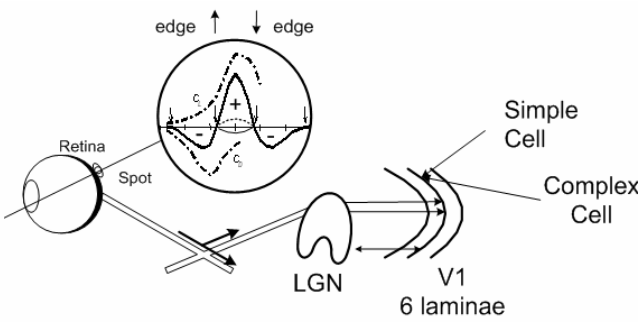

Figure 2. *Schematic of pathway from receptive fields of retinal ganglions to visual cortex V1 via LGN. Also the excitation (positive) and inhibitory (negative) effect for edge intensity of the respective on-centre and off-centre neurons is shown for one edge of a 2D spot on retina.* C_L *and* C_D *from the LV de's are both positive spike envelopes (imps/s) but their respective excitatory (+ve) and inhibitory (-ve) effects are opposite as shown to form the edge intensity result (dark line).*

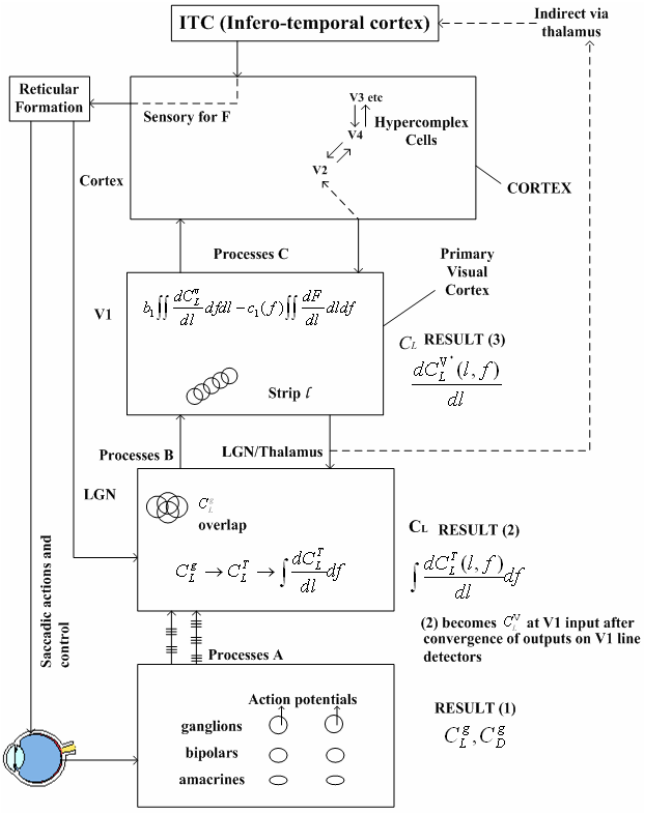

Figure 3. *Schematic representation of outputs from retina to V1 for* C_L *using functional adaptation method. Retinal processes A (see Fig 4) produce* C_L^g, C_D^g *envelopes of ganglion(g) spatio-temporal spike pattern (labeled Result 1). Processes B at LGN for convergence and overlap at LGN of thalamus T and produces Result 2. Processes C at V1 (see text) yield Result 3 for spatial gradient of* C_L^{V*} *for edge location* ℓ*. Signals in indirect link (dashed line) via ITC interact with sensory processes component* cF_i *(see text) as part of the interaction* F *for* C_L *and* C_D *in V1 laminae output and signalling exchanges with LGN.*

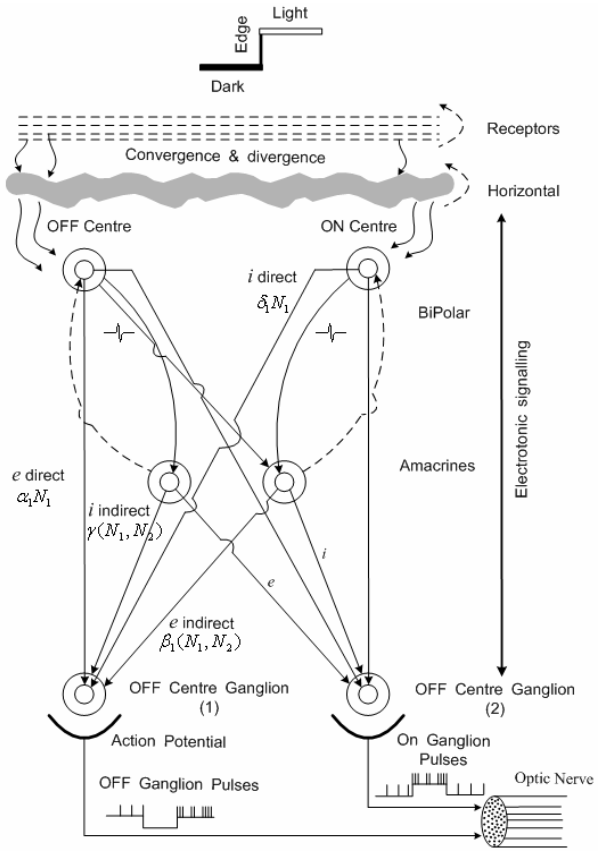

Figure 4. *Parvo signalling pathways of retinal electrotonic processes for on-centre and off-centre neurons from receptors of edge image via direct and indirect paths to corresponding ganglions for action potential discharges to optic nerve. Symbols used for the four inputs to ganglions on left side (off-centre case) of diagram: Excitatory electrotonic pulse designated* e *and inhibitory* i *in local electrotonic signalling.* $N_1 = \sum n_i \sigma_i$ *is potential strength of* n_i *inhibitory inputs of potential charges* σ_i *from electrotonic processes of activated ganglions between* $\ell, \ell + \Delta\ell$ *from bipolars and amacrines excited from the spatial retinal receptors. Similarly for* N_2 *for excitatory.* C_D *and* C_L *are proportional to* N_1 *and* N_2*. Direct input* $a_1 N_1$*. Indirect interaction* $\beta_1(N_1, N_2)$ *via amacrines has coefficient from* a_1 *and* β_1 *proportional factors from branching and interaction. Indirect interaction* $\gamma(N_2, N_1)$ *similarly formed. Direct input* $\delta_1(N_1)$ *is from inhibitory component of on-centre bipolars (right side of diagram) and adds to input for off-centre ganglions (left side). Expression for change in off-centre potential* ΔN_1*, (excitation* $E_1 -$ *inhibition* J_1*), for locally activated neurons over the increment over the increment* ℓ *to* $\ell + \Delta\ell$*, results from* $E_1 = \alpha_1 N_1 + \beta_1(N_1, N_2), J_1 = \delta_1 N_1 + \gamma(N_2, N_1)$ *.* $\Delta N_1 = (E_1 - J_1)$ *similarly* $\Delta N_2 = (E_2 - J_2)$ *.* $\Delta N_1 / \Delta\ell$ *and similarly* $\Delta N_2 / \Delta\ell$ *give the give LV format for spatial gradients of* C_D *and* C_L *to which they are proportional. The parameters controlling* C_D *and* C_L *for the edge formation are seen to be* $(\alpha - \delta), (\beta - \gamma)$ *for each LV equation.*

Murray[8]. The use of the LV analogy is applicable for our purpose because of (i) an earlier development from information theory which provides a means to incorporate "function" into components of a neurological physical information system rather than be limited to assigning "classification of tasks", (ii) published results[10 11] and more recent experimental studies[7] have shown that groups of neurons can act as single population entities in vision including the primary visual cortex. We therefore used the envelopes of the spatial responses of the on-centre and off-centre neurons as two separate species which we designate as C_L and C_D for the respective envelopes of the spike train discharges. These are shown in Fig 2 for one discharge cycle of each ganglion type. The result from the combination of C_L and C_D envelopes of discharges for light, L (positive) and dark, D (negative) spatial responses in Fig 2 is for the front left side of the small circular spot indicated on the retina. The points where the edge response crosses the spatial axis for the changes from dark $\leftrightarrow$ light are termed "zero crossings". Their importance is that a surprising theorem by Logan[12] which shows that the information contained at these edge intensity inflexions is all that is needed to define the intensity distribution. We found that its application to the zeros (ie inflexion) of second derivations of our C_L and C_D responses from the functional model diagrams in Fig 3 and Fig 4 form two LV type differential equations (shown below) for those two opposing species C_L and C_D of positive and negative excitation and their interaction via function F to form an edge. (The correspondence of inflexions of the C_L response with zero crossings of intensity can be seen in Fig 2 marked by vertical arrows).

$$a_1 \frac{\partial C_L}{\partial \ell} = b_1 C_L - c_1 F(C_L C_D)$$

$$a_2 \frac{\partial C_D}{\partial \ell} = -b_2 C_D + c_2 F(C_L C_D)$$

The spatial gradients govern the acutance and acuity for the image as seen by the observer. The formulation is given in later sections to follow but in principle, for C_L, it can be seen that the spatial rate of increase of excitation near the dark to light edge is proportional to C_L and its interaction with the inhibitory C_D is expressed by the function $F(C_L C_D)$. The corresponding equation for the spatial rate of change of C_D for the inhibition has those signs reversed from those for C_L. The resulting effect over the edge region is seen in Fig 2 and gives the "Mexican Hat" shape across a two edge region. The small drop in intensity just before the edge is advantageous for perception because of the accentuation for the boundary (Mach effect). Validation of the computed LV responses by comparison with known retinal ganglion responses for an edge is shown in Fig 5.

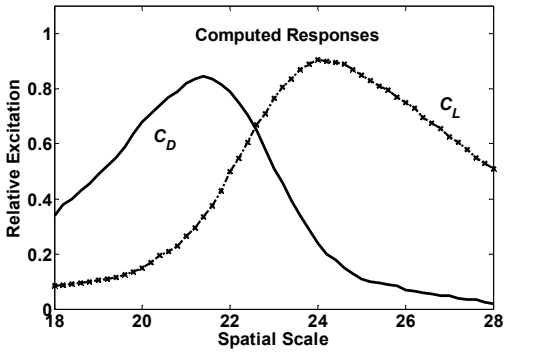

(a)

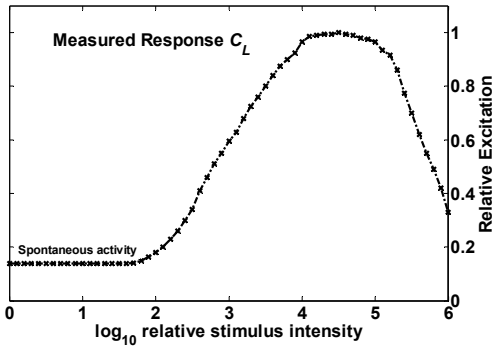

(b)

Figure 5. *(a) Computed Lotka-Volterra spatial responses for retinal ganglion responses C_L and C_D across a single dark-to-light edge. The pair of coefficients used were $0{\cdot}5, -1{\cdot}5; -0{\cdot}2, 1{\cdot}0$ for comparison across an edge corresponding to Fig 5b. (b) Experimentally measured ganglion response for turtle as a function of stimulus for retinal on-centre ganglion corresponding to C_L in Fig 5a.*

Our formulation allows for the known separate large cell magno (M) and small cell parvo (P) (for detail) pathways for on-centre and off-centre signals initiated from the respective action potential discharges of M and P type ganglions. The discharge signals proceed via the lateral geniculate nucleus (LGN) and ipsolateral and contralateral pathways to interact at V1 as shown in Fig 2 for the ipsolateral path. We introduced computer software generated noise using dynamic polaroids (Fig 1) into the early vision pathways via the retinal receptors from dynamic polaroid fields for power spectra requirements. The $1/f$ noise sequences interact with the two signal trains C_L and C_D in V1 according to the stochastic resonance properties[3] of the two LV de's for the two variables interacting with $1/f$ noise at V1. We examined the amplitude and frequency of occurrences of combinations of C_L and C_D in a 3 dimensional plot of orbital responses over 500 repetitive discharge cycles during an observer's inspection as will be seen later in this paper (Fig 7) where time dependent higher resonances are shown to occur at small value combinations of C_L and C_D, ie at weak edges.

Reference set of images and their ratings

A reference set of mammogram images from breast mammograms regions of interest was provided from a hospital breast clinic data base in order to present a range of edge detail in shape, sizes and optical density of separated clusters (which can be quantified) of small white or gray microcalcification deposits (approximately 0.1 to 1mm) as viewed by radiologists in regions of interest for early signs of possible breast cancer. However our experiments were just for edge dependent detail not the expert requirement for diagnosis for earliest signs of possible breast cancer.

An experienced breast radiologist was used as a control for ratings (1-5) to be made on edges based on shape, size, density and distribution of the microcalcifications. His ratings were then compared with a calculated fractal dimension of each of the corresponding regions using a method which includes the pixel grey level and also accounts for size, shape, density and distribution[13]. The comparisons of fractal dimensions ranges with the radiologist's ratings in the ranges 1 to 5 showed consistency. Cluster analysis showed that all the ratings for the 30 individual cases, when plotted against the fractal dimensions, showed values of connectedness (mean squared radius MSR) consistent with the 1 to 5 rating scales. In other words the less experienced observers' visual ratings for edges for shape, size and density could be compared with verified known reference levels. This supported our use of observer ratings for the detail.

We used two groups of five independent observers all of whom were from different backgrounds and had no communication with each other. They all had basic levels of experience with other types of images, not microcalcifcations. The observers were shown a range of separate image cases with edge dependent detail which had been rated as 1, 2, 3, 4 or 5, by the experienced radiologist. We showed these differing introductory images for several minutes before beginning the actual tests on the 30 cases. For the experiments each observer was told that they would be asked to rate each test image presented as 1 to 5 based on clarity of edge dependent detail when noise or no noise was applied (out of sight) in random sequences. They were not told of any possible difference. This also applied to our experienced radiologist who participated. Performance in relation to noise application was not amenable to Receiver Operating Characteristic (ROC) measurement where observer decisions are plotted in relation to a definitely known result, as in diagnostic tests. The observer tests and results are presented in Sections 5 and 6 following our new method of generating $1/f$ noise for use in the observer vision system.

Generation of the $1/f$ noise

Various methods for generating $1/f$ noise time series have been proposed in the literature including half-order integration of white noise[14], fractal-like division of the

space[15] and the sum of fluctuations with different relaxation times[16].

We generated $1/f$ time series (Fig 1) based on another known principle[17] with a white light source and tuned filters which we implement with two crossed eyepiece polaroids and a dynamic, randomly stepped swinging Polaroid. This provided independent random segmented inputs in time to a separate multi-spectral filter in each eyepiece, giving different maxima in each case between the declining yellow (filter 1) and blue (filter 2) colour-opponent neuron responses in that visual range of approximately 600 - 400 nm . Colour opponent neurons can discriminate wavelengths independent of brightness such as produced by the crossing of the dynamic polaroid sheet in the system of Fig 1. The frequency deformation with spectral power correlations needed for the $1/f$ noise were provided by the known overlapping correlated spectral absorption response correlations between rod and cone retinal receptors over the wavelength range. Each eyepiece also had a polaroid included with its plane of polarisation orthogonal to that of the other eyepiece. The combination allows different groups of wavelengths $\lambda(t)$ to be inputs for each eye dependent on the axis of orientation of the main polaroid when swinging (swing times of the order $0.1s$, across an edge region of approximately $\pm 1^0$ of retinal angle). The adjustable separate eye pieces with polaroids and filters for the left and right eyes were fitted to a light box with black interior. When the polaroid is moving in random stepping transits across the optic axis, each eye is subjected to segments of random time sequences of differing, but correlated, wavelength segments over its particular filter's spectral response. These independent inputs are analogous to a sequence of responses from tuned filters[16] in electronics. Each filter provided declining transmission coefficients, T, in the ratio 10, 5, 2.7 (approximately) at their turning points. The overlapping correlated responses of the three retinal cone types L, M and S and the rod peak response (498 nm) located between the M and S cone responses are the sources for the correlated power spectra required. As a result of the overlaps of their correlated spectral responses curves and the swinging Polaroid and eyepiece filters, the original white noise input spectrum acquires correlated power spectral correlations which decline approximately in the form required for $1/f^{\alpha}$ type noise. (α was calculated[17] as approximately 1.3).

Observer tests

The first test series (A) test used ratings (1 to 5) of detail clarity (poor to quite clear) for observation in two randomised presentations of the 30 images without and with noise added in randomised sequence. The experiments were undertaken with the understanding and consent of each observer. The control system was out of sight of the observer.

A sample size of 30 was the requirement[18] for a one-tail test to compare two series of randomised image observations for 2 groups (Series A and a subsequent Series B) each of five observers. Series A presentations for detecting a difference with 80% probability of success at a 95% confidence level, were one with noise, the other without, in random sequence, Series B used "with noise" and "with placebo" (known with harmonic perturbation) in random sequence. A one-tail test was used, being better for disclosure of a difference[19] when, on theoretical grounds, an assumed difference is thought to exist and is justified when the nature of the difference may be for reasons other than those connected with the actual samples (ie $1/f$ noise added or not). A rating of 1 to 5 for detail was required within a period of approximately 30 seconds for each image presentation. Series B was a more stringent and more experimentally symmetric and less subjective than Series A, using an alternative forced choice (AFC, better, worse, no change).

Photometric measurements of the light intensity levels at the eyepieces for both modes of operation were used to calculate the incident light flux. This was done in order to compare with published data[19] on the effect of changes in intensity as the dynamic polaroid in Fig 1 passed across the static polaroid in each eyepiece. It was shown that the rates of change of intensity in the experiment were considerably less than the level which produces any noticeable increase in optic tract activity. Optic tract activity from intermittent light flux is known to be mainly in the magno pathway but the parvo pathway is the basis for spatial detail as mentioned previously in our Theoretical Background.

Also, for visual sensation and visual acuity at levels of retinal illumination within which the observations were made, (approximately 0.01 lumens/ m^2), published data shows that the effect of changes in illumination as the polaroid swings, corresponds to the almost flat linear range for changes in visual acuity[21], as previously mentioned. In other words there should be no difference due to temporal changes in illumination in the observer's acuity between the two modes of observations in the two motions "with $1/f$ noise" and the harmonic placebo perturbation used in the Series B tests. The changes in "brightness" due to the polaroid motion in both cases were of the order $20\mu V$ rms and $10\mu V$ rms and we note that spectrally opponent cells can discriminate wavelengths independent of brightness[20].

Results of observer tests

The results (Sign Test) for the A Series gave $p < 0.05$ (A Series) for the 300 observations from two sets, each with 5 observers x 30 randomised presentations, each observer making observations and ratings in real-time with and without the noise randomly applied. In the less subjective alternative forced choice (AFC) B Series, 7 of the 10 observer results sets (5 observers, 2 sets) gave $p < 0.07$. In those 300 AFC observations (Table 1) 59.4% preferred the image detail with added noise, 22.3% no change and 18.3% chose without noise.

Table 1. *Series B observer results.*

Order for 'noise added'	No change	Better	Worse	All
2nd	22	87	21	130
1st	45	91	34	170
All	67	178	55	300

The experienced radiologist, included in each series, gave $p < 0.01$ for his separate results in both series A and series B. One observer in the B Series (AFC) had almost no experience in examining images for detail and was unsure of his choices, occasionally requesting repeated presentation of an image. His performance was the main contributor to a few poor results. Opinion from the Clinical Trials Unit at the University of Sydney was that that the main results $p < 0.07$ should not be rejected in view of the number of observations (Series B, Table 1) and the number of positive effects recorded plus the bio-neurological nature of the experiment and the advantage of experience versus little experience with detail in images. Extensive statistical analysis of the observers' results showed no affect of visual tiring and only a marginal statistical difference regarding the order in which noise was randomly presented with noise (87/91). The result for intraobserver variability was at the $\kappa > 0.4$ level for both Series A and B but interobserver results were more variable $\kappa << 0.4$ probably due to the quite different types of work experience with other types of images. Also the images used were from analog mammogram systems and better contrast is now available from digital systems entering breast clinics. Nevertheless there are always cases with weak edges.

We were surprised at statistics from a national sample experiment in the United States where experienced radiologists were sent a set of mammograms to search for features for diagnosis. When the same unidentified set was sent to the same observers several months later, there was a variability in their results of up to 11%. In our own experiments it was shown that the observers were all different from each other $\left(\chi^2\right.$ test for bias), as would be expected, since they were all selected from different backgrounds and with different types of image experience. However, our interest was for any effect on the observer's perception when an image was presented with noise.

The importance of an organised spatial search method will be seen from the results of our model where it will be shown that a spatial search is needed rather than relying on an overall observation expecting details to 'stand out' in an overall static observation (which is not uncommon). This is recognised by experienced radiologists and from observers' methods noticed in training sessions.

Theory supporting the information based methodology and results

We now provide more details of the modeling used in the project and explain specific observer dependence in the different approach to the usual micro-network complexities. We begin with the use of the two interacting species for the edge formation at the retina and then proceed to the primary visual cortex V1 where we develop the expression for the edge at that location and the role of observer attention. A "two interacting species" model of edge formation from incident light flux I used the two excitatory and inhibitory edge responses represented by the spatial envelopes represented by $C_L[I,\ell,\lambda,t]$ and $C_D[I,\ell,\lambda,t]$ of the respective frequency modulated spike discharges (imps/s) originating from the particular groups of retinal ganglions being activated across the dark(D) to light(L) edge region ℓ. Together, the C_L and C_D envelopes form the "Mexican Hat" shape of edge response for a retinal spot image (Fig 2). The edge acutance is dependent on the spatial gradients of C_L and C_D at the zero crossings (from dark $\leftrightarrow$ light) of the edge intensity response.

The modeling of many of the very complex vision processes is a challenging task. However, neurobiology of vision is a type of information system and the spatial envelopes C_L and C_D of the spike discharges contain the information for edge formation[12]. An extension of information content in Information Theory for functional classification[23], originally developed for bacteriology, prompted our new method for representing functional entities producing the information for an edge response. The usual expression for information content in information theory applies to ability but not to function[24] which is particularly important in biological and neurological applications. Our adaptation for a function based edge model was formatted from the description of functional pathways[25,26] and the need for segregated information systems in vision to be accessible to integration at every stage[25]. The complexities of vision processes limit our modeling to a simple image edge environment

For our purpose it overcomes the functional shortcoming which has been cited[25] as such for earlier *task-based* edge modelling of Marr and Hildreth[27]. We use information content as defined ex novo by Resigno and Maccacaro[23] based on a hierarchy of functional properties, not their similarity. It is a method whereby a group of operators (eg mathematical) is the basis for classifying a set of entities into a number of subsets where each subset consists of functions which do not differ in themselves as a group but are different from those in other subsets by at least one of the operators. The functional subsets then formed have been called "formae" (from J. Steiner in Gesampte Werke Vol 1, 1832). Further detail is found in the Resigno and Maccacaro reference[23] for the principles used at each stage of early vision in our model. From the established principles of early vision and the foregoing method. It allows identification of the functions involved for our edge model which then relates acutance and acuity for observer performance with a minimum number of variables and parameters.

By applying the foregoing method into the signaling pathways at each physiological level of the early vision

pathways (Fig 3) we can express functions of C_L and C_D consistent with Marr and Hildreth conditions for an edge[27] and envelopes[28]. These functions are continuously dependent on the data even though there can be digital $\leftrightarrow$ analogue conversions of the signals by the known properties of neurons.

The responses C_L and C_D in the resultant information processes shown in Fig 3, apply particularly to the parvo pathway for detail, as previously mentioned. The parvo P (small cell) pathway in the human visual system begins in the P type ganglion cells of the retina and ultimately divides to form the pathway for colour and small detail and a magno M (large cell) pathway is mainly for 'form' and motion. Specialised visual areas of the cortex can make use of both types of information. Within the cortex the M and P the signals can mix and the inputs to the specialised visual areas utilise signals from either source[26].

Beginning at the retinal stage we are dealing with "simple" cells with well-defined excitatory and inhibitory subregions of their receptive fields. They respond best to lines or edges and our subsequent edge formulation at V1, (to follow) allows us to obtain the spatial gradients of C_L and C_D at V1 across an edge region ℓ. At that stage the zero crossings from their inflexions corresponding to light $\leftrightarrow$ dark transitions at an edge yield LV type de's. We can then examine the responses when $1/f$ noise is added in the model over repetitive temporal cycles of C_L and C_D. We firstly proceed to formulate the initial C_L and C_D edge responses at the retinal ganglions.

Retinal signalling

Fig 4 shows the direct and branching pathways[25,26] used in the formulations to obtain the action potentials for C_L and C_D at the retinal ganglions from the excitatory and inhibitory electrotonic interactions at the edge-activated groups of neurons in the preceding retinal layers. It has recently been shown[29] how the interactions govern the resulting ganglion spiking pattern. The envelopes of the pattern correspond to our C_L and C_D envelopes.

Fig 4 shows the proportional content of the initial spatial signals for an edge arriving at the associated destination of on-centre and off-centre ganglions directly or by branching via the electrotonic signals of the horizontal (mediating) cells, bipolar and amacrine cells. The direct and branching pathways between the on-centre and off-centre receptive fields of the cells[25] provide the branching signaling diagram for destination distribution at the activated on-centre and off-centre ganglions. The resulting action potentials from the respective activated ganglions provide the subsequent excitatory and inhibiting pulse signal spikes to the optic nerve. These frequency modulated pulse signals carry the spatio-temporal edge response information to the lateral geniculate nucleus (LGN), a small but important part of the thalamus is still not yet fully understood.

Interaction of the two species of signalling for retinal ganglion responses

In the excitation and inhibition processes of convergence and divergence of connections in the signaling pathway, the spatial rate of change at a given stage is proportional to the number of cells influencing it at that location and to the number of the interacting excitatory inhibitory cells. This is shown by the parameters a, β, δ, γ in the legend to Fig 4. The potentials are additive but the number of possible interacting cell signals N_1 and N_2 is proportional to the product $N_1 N_2$ (similar to the interaction of species in Lotka and Volterra models[9]). The interaction of a single excitatory signal pulse e with an inhibitory one i at the same spatial location for edge response requires these two signals $i(\ell, t)$ and $e(\ell, t)$ to correspond closely in location and time t at the particular retinal cell. We can express this requirement in terms of a windowed correlation $\int_{-\infty}^{\infty} e(\ell) i(\ell - \Delta) d\ell$ between them[17] over a small spatial length Δ in the duration of a single electrotonic signal pulse. The resultant interaction is of a product form but the exact function is not known. However, we will see that our response results (Fig 5a) show that the simplest product form for the interaction term in the LV equations yield responses for an edge from the beginning of the ganglion activation period, consistent with ganglion potential measurements[30] in Fig 5b. The changes in potential encountered at an edge are compatible with the excitation levels corresponding to our C_D and C_L values.

The computed responses in Fig 5 were obtained for that comparison by using appropriate coefficients for a realistic three decade exponentially rising spatial edge intensity beginning with the edge activation of ganglions. The two variables N_1 and N_2 in Fig 4 represent the total of the output strengths of the off-centre and on-centre ganglion potentials across the edge region and are proportional to C_D and C_L. Formulation in this way[31] yields a set of LV type differential equations for a simple edge model as summarised in the legend for Fig 4. They apply for each spatial frequency channel f_i. The retinal ganglion coefficients $\alpha - \delta$ and $\beta - \gamma$ in the LV equations relate to acuity via their representation for the spatial rate of change $\Delta N_1 / \Delta \ell$ and $\Delta N_1 / \Delta \ell$, ie the spatial rate of change of inhibition and excitation which together form the shape of the retinal edge response along the region ℓ.

The short linear inactive discrete time between discharge cycles does not affect the cyclic LV repetition property[32] of the spatial envelope patterns of potentials and ganglions discharge spikes over the same length ℓ of the repeated ganglion activity for the edge. As will be seen below, a class of LV responses for an edge is also generated at V1 and this is consistent with the conformal shape-preserving retinotopic property of the early vision system.

Interaction of C_L and C_D sequences at V1

From the retinal ganglion input to the LGN, most signalling information goes to V1 but some proceeds via the thalamus to the infero-temporal cortex (ITC) and held in short term memory accessible to subsequent V1 exchanges with the LGN. Retinal spatial frequency selectivity increases in the LGN from signals exchanged back from selective cells in V1. Information from the overlapping of retinal responses at the LGN stage is not utilised until interactions at V1 take place with complex cells as indicated in Fig 3. "Complex" cells (with complex OR operation) can fire to stimuli from both "simple" (with AND operation) and other complex cells. A complex cell has been modelled[33] within experimental ranges as a coincidence detector in encoding synaptic events within a time window of the order of 2ms from simple cells. This is consistent with our input times from the left and right eye. Although individually, the complex cells appear to be insensitive to phase, the information content of their group populations has been shown[34] to contain sufficient information for capturing the perceptual essence of images for identification in a robust manner. Information encoded in time across ensembles of synchronous neurons converges to single neurons downstream in the visual pathway and we therefore assume that the original temporal noise can interact with the C_L and C_D information brought together at V1.

At V1 the C_L excitatory and C_D inhibitory signal components are interacted[27] and are represented in our proposed interaction process (Fig 6a,b) which originated as follows. Siegal[9] examined the encoded inter-spike interval data for the dynamics of single unit activity of groups, O(10^4), of single neurons in the primary visual cortex of the cat. He suggested that the dynamics may be "not highly complex" despite the highly complex system itself and possibly modelled by a "small set" of coupled nonlinear equations, as we have found. The advantages of modelling larger scale neuron activity which exhibit a coherent group organisation were subsequently discussed by Sirovich et al[11]. No model was presented but organising principles for analysing and viewing data were presented. In our model, V1 laminae interactions of C_L and C_D components are obtained for any particular region by using a cyclic convolution of present and previous spatio-temporal signal components (Fig 6b, *e* and *g*) of sequences S(E) and S(G) of the spatio-temporal C_L and C_D signals. As seen in Fig 6b the n interaction components in the signal train for the interaction are of the form $\sum_{k=0}^{n} a_k g_{n-k}$. This process meets the requirement[35] for speed of signalling to other regions of the visual cortex and also provides for retinal shift invariance[36] using the summations for cyclic time displacements of the bilinear $C_L C_D$ products[37] as shown in Fig 6b. This is consistent with the fact that the visual areas are not connected serially with each other as is known medically from specific visual defects.

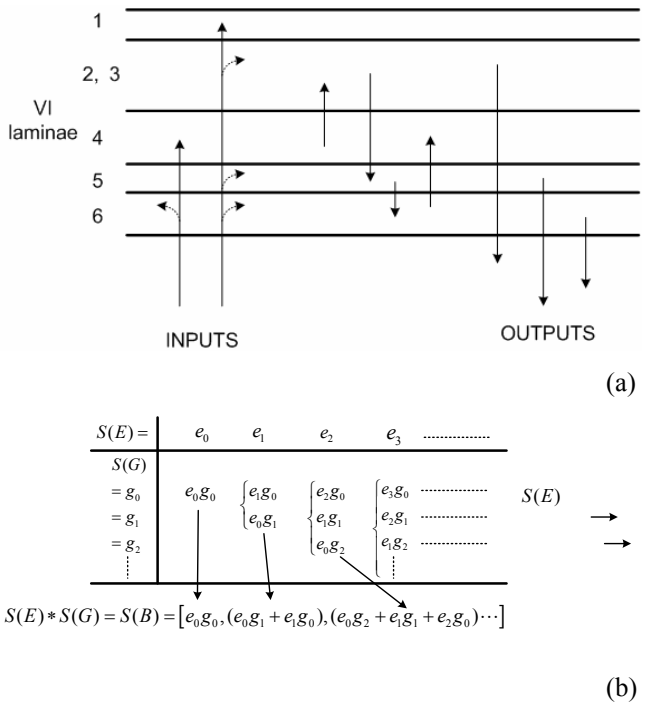

Figure 6. *(a) Grossly simplified diagram for some of the known main pathways within visual cortex V1. (Laminae connectivities still not all known). Adapted from Crick 1994. (b) Algorithm representation for cyclic convolution principle of two spatio-temporal sequences S(E) and S(G) corresponding to C_L and C_D signal inputs to V1. Successive temporal displacement of one sequence allows a rapid linear additive operation for bilinear products of current and previous interaction components.*

The neurons in V1 laminae can transfer the signal train of sequences of C_L and C_D components of the activated groups of neurons into a spatial pattern with one-to-one correspondence between temporal and spatial configurations for conditions[38] which are complied with in our model and our experimental system such as limiting the size of inputs. This was first illustrated in principle with computer graphics in an early computer network experiment[38] with "neuron-like" computer components and with quantitative support for applicable conditions. Since then there have been related transfers noted in neural net studies of patches of cortical neurons which are dynamic in time but have a simplified spatial response[39 40]. Temporal-to-spatial processes have been supported by recent work (tracer substances injected) and a relevant diagram is also shown in a cortical review[40].

Zero crossings for equations for edge formation at V1 including observer attention

At V1 we used the theorem by Logan[12] which shows that the information contained at the edge intensity inflexions (zero crossings) is all that is needed to define the intensity distribution. Observer perception depends, in part, on the sharpness of an edge and is therefore related to intensity gradient close to the zero crossings[27]. As will be seen below, in Eq(1) and Fig 3, our information based

formulation can provide the gradients from the difference between the expression for V1 outputs C_L^{V*} and C_D^{V*} and the relevant inputs for C_L^V, C_D^V in terms of the processed information[31] for their interaction at V1. If two synapses are close together on a thin dendrite, the conjoint firing of the two classes of input allows the dendrite to sum the products in the bilinear form[37] $F = \sum m_{ij}\, C_{Li}\, C_{Dj}$ where m_{ij} represents the i, j synapse connection strengths. The vision system requires integration at every stage[26] and is a multi-step process. The resulting on-centre result at V1 is consistent with the adapted information theory requirements of Rosigno and Maccacaro[23] (processes labelled C at the V1 cortex in Fig 3).

$$\left[\frac{\partial C_L^{V*}}{\partial \mathrm{l}} - a_1 \int_i \frac{\partial C_L^V}{\partial \mathrm{l}}\, df\right] = H_L \text{ where}$$
$$H_L = b_1 \int_i \int \frac{\partial C_L^V}{\partial \mathrm{l}}\, d\mathrm{l}\, df - c_1(f_i) \int_i \int \frac{\partial F}{\partial \mathrm{l}}\, d\mathrm{l}\, df \tag{1}$$

This applies for each spatial frequency channel f_i (not related to the usual f nomenclature for "$1/f$ noise"). Similarly for the off-centre case giving a complementary equation:

$$\frac{\partial C_D^{V^*}}{\partial \ell} - a_2 \int_i \frac{\partial C_D^V}{\partial \ell}\, df = H_D \text{ where}$$
$$H_D = -b_2 \int_i \int \frac{\partial C_L^V}{\partial \ell}\, d\ell\, df + c_2 \int_i \int \frac{\partial F}{\partial \ell}\, d\ell\, df \tag{2}$$

In the off-centre equation the output for a dark-to-light edge response spatial gradient $\frac{\partial C_D^{V*}}{\partial \ell}$ is negative when the on-centre response gradient $\frac{\partial C_L^{V*}}{\partial \ell}$ is positive at a zero crossing at or very near the actual edge boundary[27]. The right hand side of the equation is then of opposite sign to that of Eq(1). Superscript V applies for information input and V* for output information. Lateral linking interactions could be included in our model if known, such as occurs in lamina 5 and on to lamina 6. Also, with some simplifications and limitations we can see (but not studied) a possible LV relationship of our "two species" approach, to a two species excitation and inhibition firing rates model[42] using mean-field equations which simulate only lateral excitations.

The coefficient c for the interaction term in Eqs(1) and (2) is $c = \left[1 + s(f_i)\right]F$ to provide the linear additive observer's selective inhibition ability by including the spatial frequency function $s(f_i)$ for observer attention. It results from the known ability of observers to suppress unwanted detail in complex images as shown from *fMRI* experiments[43]. The effect arises from the observer's cerebral functions associated with the observer's attention via the inferior temporal cortex (ITC) and the psychophysical feedback from the reticular formation located at the top of the brain stem. We also noted[39] the role of an observer's attention in the control of information processing in functional reorganisation of spatial frequency filtering of the receptive fields. Those cited experiments support the incorporation of $s(f_i)$ in our interaction formulation using the adaptation of information theory for function whereby identified levels of activity can be treated independently. The numerical value of the function is not known but its existence is important although relatively small since, for a real edge, the zero crossings for different spatial frequencies should be "not too far apart" for a real edge, to quote Marr and Hildreth[27].

The two equations (1) and (2) yield two de's after differentiation under the integral sign with respect to ℓ using discrete step function selective spatial frequency thresholds[44] for the f_i. The second differentials for each f_i channel are:

$$\frac{\partial^2 C_L^{V*}}{\partial \ell^2} = K_L \text{ where } K_L \text{ is}$$
$$a_i \int_i \frac{\partial^2 C_L^V}{\partial \ell^2}\, df + b_1 \int_i \frac{\partial C_L^V}{\partial \ell}\, df - c_1(f_i) \int_i \frac{\partial F}{\partial \ell}\, df \tag{3}$$

$$\text{i.e. } \frac{\partial^2 C_L^{V^*}}{\partial \ell^2} = \int_i \left[a_1 \frac{\partial^2 C_L^V}{\partial \ell^2} + b_1 \frac{\partial C_L^V}{\partial \ell} - c_1(f_i) \frac{\partial F}{\partial \ell}\right] df \tag{4}$$

A similar set of differential equations is obtained for $C_D^{V^*}$

$$\frac{\partial^2 C_D^{V^*}}{\partial \ell^2} = \int_i \left[a_2 \frac{\partial^2 C_D^V}{\partial \ell^2} - b_2 \frac{\partial C_L^V}{\partial \ell} + c_2(f_i) \frac{\partial F}{\partial \ell}\right] df \tag{5}$$

The second differentials $\frac{\partial^2 C_L^{V^*}}{\partial \ell^2}$ and $\frac{\partial^2 C_D^{V*}}{\partial \ell^2}$, are zero at the inflexions of the variables at zero crossings, the result from which when equated contains the information for the edge intensity distribution[12]. We know that the integrand of the right hand side of Eqs(4) and (5) and is not an arbitrary function which might be equated to zero to meet that condition. It must conform to a shape of the same form of response as projected from the LGN to V1 so our expressions in square brackets in Eqs(4) and (5) is a correct candidate when equated to zero for a response at each of the spatial frequency channels. Equating the right hand side of Eqs(4) and (5) to zero therefore provides the information for the edge using Eqs(7) and (8) below. From Eq(4),

$$\int_i \left[a_1 \frac{\partial^2 C_L^V}{\partial \ell^2} + b_1 \frac{\partial C_L^V}{\partial \ell} - c_1(f_i) \frac{\partial F}{\partial \ell}\right] df = 0 \tag{6}$$

from which, for the C_L process at V1 the integrand yields

$$a_1 \frac{\partial C_L}{\partial \ell} = -b_1 C_L + c_1(f_i) F \tag{7}$$

omitting the superscript V (for notation simplicity) Similarly,

$$a_2 \frac{\partial C_D}{\partial \ell} = b_2 C_D - c_2(f_i) F \tag{8}$$

The two LV equations (7) and (8) provide the edge conditions governed by coefficients a, b, c and the interaction function F in V1 for each separate spatial frequency channel $f_i(i = 1, 2....n)$ and each has its own contrast threshold[44]. As a result of the above LV formulations the C_L and C_D responses provide the basis of edge intensity and also provide the known retinotopic property of early vision between retina and V1 as mentioned previously. The coefficients a, b and c govern the spatial properties of the solution of Eq(7) and (8). The Marr and Hildreth conditions for a true edge would be satisfied provided that the coefficients a, b, c in each channel do not differ greatly for the zero crossings for the separate frequency channels. Depending on the image quality of an edge region and observer attention function $s(f)$, the associated coefficients c_1 and c_2 may be slightly different for each channel and result in small changes in the responses which then lead to small displacements of the zero crossing points. The responses C_L and C_D in LV equations cannot be obtained in closed form and must be computed, as done for Fig 5. However, the orbital equation for C_L and C_D is easily found and it is of more value for our purpose of revealing edge responses from the joint occurrences of these two variables when interacted with $1/f$ noise (as shown in Fig 7). This will be seen in the following Section.

Orbital representation of C_L, C_D show resonances for weak edges

Eq(7) and Eq(8) can be used in the usual text book manner to obtain the basic orbital equation(9) below for plotting of C_L versus C_D for repeated cycles from ganglion discharges. We wished to plot the relative density of occurrences of C_L and C_D values on the vertical axis for their values on the X and Y axes to see the distribution of approximately equal joint occurrences required for an edge.

$$\frac{\partial C_L}{\partial C_D}\left[-a_2/C_L + c_2 F\right] = (b_2/b_1) C_L \left[a_1/C_D - c_1 F\right] \tag{9}$$

In Fig 7 computer generated $1/f$ noise $\psi(\ell, t)$ was added to each of the spatial variables C_L and C_D using the multiplier $1 + \psi$ which then simulates the experimental system for $1/f$ noise interaction with C_L and C_D corresponding to its affect in the function $F(C_L, C_D)$ at V1. When the noise term is added in this way in Eq(9) integration with respect to ℓ gives the orbital spatio-temporal values of C_L and C_D across ℓ for the successively plotted responses across successive discharge cycles. The result of 500 discharge cycles is shown in Fig 7. As in the retinal responses of Fig 5, a simple bilinear interaction function was used in our computation for noise interaction in F and we used the same values for coefficients a, b and c as used for corresponding coefficients for excitation and inhibition in the retinal LV for results in Fig 5.

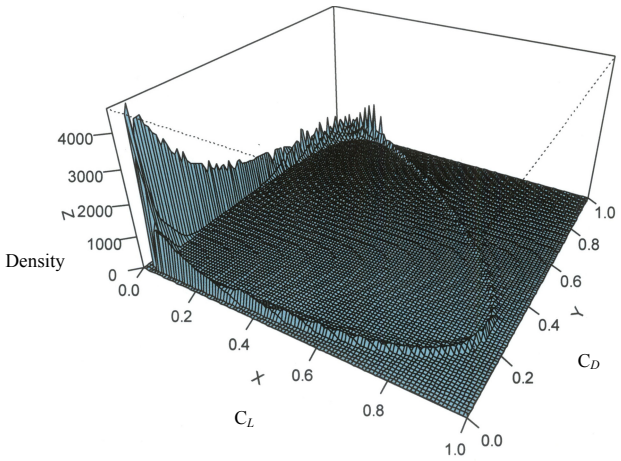

Figure 7. *Typical repetitive orbital computer plots (500 cycles) for C_L and C_D trajectories (X and Y axes) showing cumulative density of occurrences (vertical axis) of combination values corresponding to one spatial frequency channel and with simulated $1/f$ noise in C_L and C_D using bilinear $C_L C_D$ terms in F. Maxima and minima densities are higher at smaller values of non-stationary C_L and C_D and indicate underlying SR effect for improved weak edge perception when scanning an image. The approximately equal values needed for edge formation occur at separate threshold levels[44] ie in two dimensional planes containing approximately equal C_L and C_D values. Orbits shown correspond approximately to the time for observer decision in the experiments.*

In the orbital responses in Fig 7 we see sharp peaks in the density of occurrences (vertical axis) of C_L versus C_D instead of otherwise smooth cyclic curves at a lower level without noise. When the peaks for C_L and C_D occur reasonably close together, as required for an edge, as seen in Fig 2, any sharp non-stationary peaks above an observer's threshold level provide an increase in edge perception and acutance. The main peaks occur at small values of C_L and C_D (ie at weak edges). The peaks as shown would also initiate signals from V1 to LGN/thalamus with high pass filtering in the thalamus[45] to produce non-stationary saccades for observer attention via the recently confirmed thalamus link to the frontal cortical neurons[3].

Discussion

The peaks and troughs in the spatio-temporal orbits were found to be not stationary, neither spatially nor temporarily, as opposed to an earlier computational LV study which indicated stationary "preferred orbits" for a case which had $1/f$ noise added to just one of the two variables in only one of two LV equations. A subsequent study[3], in conjunction with that original author, showed that the apparent stationary property may not have been correct, possibly due to a computational process used for the $1/f$ noise. However, in those papers and in our present study, the peaks were stated as indicative of an underlying type of stochastic resonance[3 47] and the non-stationary property which we now suggest can explain our experimental results and improved edge acutance for detail in most of our observers when scanning in an orderly manner.

Acutance is a measure of the sharpness of an edge expressed in terms of the mean square of the gradient of luminous flux (or image density in a film image) with distance from the edge. Acutance and resolving power (in acuity) are often closely related but this need not be the case. Acutance, A, has been often used as a measure of the image quality but it is known that the expression $A\left[1-\exp\left(-kR^2\right)\right]$ is well correlated with subjective impressions of the image sharpness[46]. k is a constant and R is resolving power. This aspect of observer dependence is probably a contributor to the difference in edge detection performance of our observers who come from different levels of experience in viewing images in various applications in their work.

Conclusion

The functional approach to the modelling from retina to V1 for edge detection was made possible by the fact that C_L and C_D and the mathematical operations on them, conform with the requirements for "information content" from Shannon's Information Theory, as extended for *functional* operations[23]. For our simple edge model it avoids circuit-type modelling and microcircuits.

Our model and experiments are related to aspects of observer performance through the relative magnitude of the coefficients in the expressions for C_L and C_D and for the effect of $1/f$ noise in their interactions for $F\left(C_L C_D\right)$ in V1. The noise interactions based on single cell behaviour of groups of neurons[10 11] together with more than the required small number, O(10), of separate V1 multilevel threshold weak edges can produce non-stationary stochastic resonances including those for some sub-threshold levels[47]. We suggest that resonances are induced in the geniculostriate system for non-stationary peaks of combined C_L and C_D responses, especially for small values of C_L and C_D occurring together (ie in V1 at weak edges). The non-stationary resonances can provide saccade triggering from the high pass filtering in the thalamus[45]. This would occur from the effect of the $1/f$ noise when an observer spatially scans an image for edges in an organised manner. The latter aspect is a well known problem in practice if not done carefully when scanning a series of complex breast images in real-time conditions. It has important clinical implications for conjunction searches[48 49] of features in medical images including faint stellates in breast screening images, to be discussed in a subsequent paper as mentioned in the text. As mentioned previously, the independent clinical trials reviewer of our laboratory system stated that the forced choice Series B results of Table 1 $\left(p=0.07\right)$ should not be discarded in view of the neurological nature of the problem, the number of observations and the percentage of cases which gave a positive result. The Series A results gave $p<0.05$.

The principles used in the laboratory equipment can be incorporated in much smaller systems in medical applications and, with modifications (magno pathway), in other areas such as detection of objects in poor night vision conditions for vehicles. The laboratory system is not suitable for such applications or clinical usage but the designs being considered can use electro-optics and avoid the mechanical aspects of our laboratory system. A clinical system can use a conventional screen display, electro-optics and fibre optics. The application for assisting a vehicle driver in poor visibility conditions may use a projector to radiate ahead of the vehicle and a detector system for screen display similar in size and position to current car navigator systems.

Acknowledgements

We thank Breast Screening NSW for providing images to test for a range of edge detail. Dr Loraine Holley, School of Physics, University of Technology Sydney, gave valuable advice in the experimental procedures. Polaroids and related advice were provided by CSIRO Measurements Laboratory, Sydney. Expert radiologists Dr Warwick Lee and Dr Mary Rickard provided important comments from training of observers. Dr Lee also participated in our experiments. We also thank Paul Newman, NHMRC Clinical Trials Centre, University of Sydney for carefully reviewing our experimental procedures and results.

References

1. Hung, W., Nguyen, H., Lee, W., Rickard, M., Thornton, B. and Blinowska, A., *Diagnostic abilities of three CAD method for assessing microcalcifications in mammograms and an aspect of equivocal cases decisions by radiologists,* Australas. Phys.Eng. Sci. Med. 26, 78-83, 2003.
2. Kitajo, K., Nozaki, D., Ware, L.M. and Yamamoto, Y., *Behavioural stochastic resonance within the human brain,* Phys Rev Lett, 90, 218103-4, 2003.
3. Arnold, L., Horsthemke, W. and Stuki, J., *The influence of external real and white noise on the Lotka-Volterra model*, Biomed Jl 21, 451-471, 1979.

4. Sommer, M.A. and Wurtz. R.H., *Influence of the thalamus on spatial visual processing in frontal cortex, Nature,* 444, 374-377.
5. Dror, G. and Tso dyk, *Analysis and modelling of population dynamics in the visual cortex,* Neurocomputing, 26-27, 361-366, 1999.
6. Kobayashi, M. and Musha, T., $1/f$ *fluctuations of heartbeat period, IEEE,* Trans. Biomed. Eng., 29, 456-457, 1982.
7. Demanude, C., James, C., Sonuga-Bark, E., Kobayashi, M. and Musha, T., *Distinguishing low frequency oscillations within the* $1/f$ *spectral behaviour of electromagnetic brain,* IEEE Trans. Biomed. Eng, 29, 456-457, 1982.
8. Pillow, J., Shlens, J., Paninski, L., Sher, A., Litke, A., Chichiliniksky, E. and Simoncelli, E., *Spatio-temporal correlations and visual signalling in complete neuronal population,* Nature 07140 on line 23 July, 2008
9. Murray, J.R., *Mathematical Biology,* ch.3, Springer-Verlag, New York, 2002.
10. Siegel, R.M., *Non-linear dynamical system theory and primary visual cortical processing,* Physica, D 42, 385, 1990.
11. Sirovitch, L., Everson, R., Kaplan,E., Knight, B. and Orbach, D., *Modelling the functional organisation of the visual cortex,* Physica D96, 355-366, 1996.
12. Logan, B., *Information in the zero crossings of bandpass signals,* Bell Sys. Tech. J. 56, 4, 187-217, 1980.
13. Caldwell, C., Stapleton, S., Holdsworth, D., Jong, R., Weisert, W., Cooke, G. and Yaffe, M., *Characterisation of mammographic parenchymal pattern by fractal dimensions,* Phys, Med. Biol. 35, 235-247, 1990.
14. Sano, M., Nakauchi, H., Akabane, H. and Musha, T., *Model study of spontaneous discharge of a membrane potential,* Japan J. Appl. Physics 29, 2186-2190, 1990.
15. Furukawa, H., *Universal spectra of quasirandom objects produced by off-equilibrium space divisions,* Phys. Rev., A34, 2315-2323, 2000.
16. Jensen, H., *Lattice gas as a model of* $1/f$ *noise,* Phys. Rev. Lett., 90, 218103-4, 1989.
17. Crandell, R.E., *Projects in Scientific Computation,* Sections 5 and 6, Springer-Verlag, New York, 1994.
18. Al Bayyati, H.A., *A rule of thumb for determining a sample size in comparing two properties,* Technometrics 13, 75-77, 1971.
19. Diem, K. and Seldru, P.J., *Scientific Tables,* Vol. 2, 193-4, Ed. C. Lentner, Ciba-Geigy, Basle, Switzerland, 1982.
20. Pinneo, L.R., *Visual prosthesis by electrical stimulation of primary visual pathways* in Visual Prothesia, The Interdisciplinary Dialogue, 109-127 (Ed. Sterling et al), Academic Press, 1971.
21. Murch, G., Visual and Auditory Perception, The Bobb-Merrill Co Inc. Indianapolis, 1973.
22. Beam, C., Layde, P. and Sallison, D., *Variability in interpretation of screening mammograms by US radiologists. Finding from a national sample*, Achiv. Internal Medicine, 156, 20099-213, 1996.
23. Resigno, A. and Maccacaro, G.A. *The Information Content of Biological Classifications,* in Information Theory, (ed. Colin Cherry), Butterworths, London, 437-446, 1961.
24. Gilbert, E., *Information Theory and continued by Quastler, H., for Biological applications of Information Theory* in Encylopaedia of Science & Technology Vol. 5, 101 and 113-114, McGraw-Hill, New York, 1979.
25. Geisler, W.S. and Banks, M.S., *Retinal Processing* in Handbook of Optics, Vol. 1 25.10-13, (Eds. Bass, M., et al), McGraw-Hill, New York, 1995.
26. Zeki, Z. *A Vision of the Brain,* Blackwell Scientific Publications, Oxford, 1993.
27. Marr, D. and Hildreth, E., *Theory of edge detection*, Proc. Roy. Soc., London, B2007, 187-217, 1980.
28. Grussser, O.-J. and Grusser-Coornehls, U., *The Sense of Sight* in Human Physiology, Second Revised Edition, Springer-Verlag, Berlin, 237-276, 1987.
29. Roska, B., Molnar, A. and Werblin, F.S. *Parallel processing in retinal ganglion, cells: How integration of space-time patterns of excitation and inhibition form the spiking output,* J. Neurophysiol., 95, 3810-3822, 2006.
30. Baylor, D. and Fuortes, M. *Electrical responses of single cones in the retina of the turtle*, Jl. Physiology, London, 207, 77, 1970.
31. Thornton-Benko, E., *PhD Thesis, Neurological Modelling of the Vision System with Relevance to an Application for Improved Detection of Early Breast Cancer.* Faculty of Science, University of Technology Sydney, 2005.
32. Bohner, D. and Paterson, A., *Discrete Equations on Time Scales. An Introduction with Applications,* Ch. 1., Birkhauser, Basel, Switzerland, 2001.
33. Qian, Y., Xianghn, Q. and Weing, Y., *Modelling neuronal dynamic coding in primary visual cortex,* Biosystems, 58, 203-209, 2000.
34. Shams, I. and Von der Malsburt, *The Role of complex cells in object recognition,* Vision Research, 42, 2547-2554, 2002.
35. Crick, F., *The Astonishing Hypothesis, The Scientific Search for the Soul, 134,* Simon & Schuster, New York, 1994.
36. Wandell, B.A., *Foundations of Vision*, ch. 10, Sinauer Associates, Sunderland, Massachusets, 1996.
37. Koch. C., *Biophysics of Computation,* Oxford Univ. Press. Oxford, 1999.
38. Farley, B. and Clark, W.A., *Activity in networks of neuron-like elements,* in Information Theory, (Ed. Colin Cherry), Butterworths, London, 1961.
39. Dudkin, K.N., *Cooperative neural networks underlying image description in visual cortex,* IEEE Symposium on Neuroinformatics and Neurocomputers, 7-10, Vol 1, 387-398, 1992.
40. Malach, R., Avidan , G., Lerner, Y., Hansen, U. and Levy, I., *The cartography of human visual object areas,* Ch 9 in Functional Neuroimaging of Visual Cognition, (Ed N. Kanwisher & J. Duncan), Oxford University Press, 2003.
41. Syme, S., Oppwood, R., Mallot, H., Mason, S. and Zrenner, E., *Mimicking the brain*, Physics World, 15, 31, 2002.
42. Dror, G. and Tso dyk, *Analysis and modelling of population dynamics in the visual cortex,* Neurocomputing, 26-27, 361-366, 1999.
43. Carandini, M., Heeger, D. and Senn, W., *Asynaptic explanation of suppression in visual cortex,* Jl of Neuroscience, 22, 1053-1065, 2002.
44. Blackmore, C. and Campbell, F.W., *On the existence of neurons in the human visal system selectivity sensitive to the orientation and size of retinal images,* J. Physiol., 203, 237-260, 1969.
45. Beierlein, M., Fall, C.P., Rinzel, J. and Yuste, R., *Thalamocortical bursts trigger recurrent activity in neocortical networks: layer 4 as a frequency-dependent gate,* Jl of Neuroscience, 22, 237-260, 2002.
46. Higgins, G. and Wolf, R., *The relation of definition to sharpness and resolving power as a photographic system,* Jl Opt. Soc. Am., 45, 121-129, 1995.
47. Fakir, R., *Nonstationary stochastic resonance*, Phys. Rev. E., 57, 6996-7001, 1998.
48. Rolls, E. and Deco, G., *Computational Neuroscience of Vision Appendix B,* Oxford Univ. Press, Oxford, 2004.

n

49. Schall, J.D., *Neural selection and control of action. Functional Neuroimaging of Visual Cognition, Attention and Performance,* ch.20 (Ed. Kanwisher, N. and Duncan, J.), Oxford Univ. Press Oxford, 2004.